

UHRF1 Overexpression Drives DNA Hypomethylation and Hepatocellular Carcinoma

Raksha Mudbhary,^{1,2,3} Yujin Hoshida,^{1,4} Yelena Chernyavskaya,^{1,2} Vinitha Jacob,^{1,2,3} Augusto Villanueva,^{7,8} M. Isabel Fiel,⁵ Xintong Chen,^{1,4} Kensuke Kojima,^{1,4} Swan Thung,⁵ Roderick T. Bronson,⁹ Anja Lachenmayer,⁴ Kate Revill,^{2,4} Clara Alsinet,⁷ Ravi Sachidanandam,⁶ Anal Desai,¹⁰ Sucharita SenBanerjee,¹⁰ Chinweike Ukomadu,¹⁰ Josep M. Llovet,^{1,4,7,11} and Kirsten C. Sadler^{1,2,3,4,*}

¹Division of Liver Diseases, Department of Medicine, Icahn School of Medicine at Mount Sinai, New York, NY 10029, USA

²Department of Developmental and Regenerative Biology, Icahn School of Medicine at Mount Sinai, New York, NY 10029, USA

³Graduate School of Biological Sciences, Icahn School of Medicine at Mount Sinai, New York, NY 10029, USA

⁴Liver Cancer Program/Tisch Cancer Institute, Icahn School of Medicine at Mount Sinai, New York, NY 10029, USA

⁵Department of Pathology, Icahn School of Medicine at Mount Sinai, New York, NY 10029, USA

⁶Department of Genetics and Genomics, Icahn School of Medicine at Mount Sinai, New York, NY 10029, USA

⁷HCC Translational Research Laboratory, IDIBAPS, CIBEREHD, Hospital Clinic, University of Barcelona, Catalonia 08036, Spain

⁸Institute of Liver Studies, Division of Transplantation Immunology and Mucosal Biology, King's College London, London SE5 9RS, UK

⁹Rodent Histopathology Core Dana Farber/Harvard Cancer Center, Harvard Medical School, Boston, MA 02115, USA

¹⁰Division of Gastroenterology, Department of Medicine, Brigham and Women's Hospital, Harvard Medical School, Boston, MA 02115, USA

¹¹Institució Catalana de Recerca i Estudis Avançats Lluís Companys, Barcelona 08010, Spain

*Correspondence: kirsten.edepli@mssm.edu

<http://dx.doi.org/10.1016/j.ccr.2014.01.003>

SUMMARY

Ubiquitin-like with PHD and RING finger domains 1 (UHRF1) is an essential regulator of DNA methylation that is highly expressed in many cancers. Here, we use transgenic zebrafish, cultured cells, and human tumors to demonstrate that UHRF1 is an oncogene. UHRF1 overexpression in zebrafish hepatocytes destabilizes and delocalizes Dnmt1 and causes DNA hypomethylation and *Tp53*-mediated senescence. Hepatocellular carcinoma (HCC) emerges when senescence is bypassed. *tp53* mutation both alleviates senescence and accelerates tumor onset. Human HCCs recapitulate this paradigm, as *UHRF1* overexpression defines a subclass of aggressive HCCs characterized by genomic instability, *TP53* mutation, and abrogation of the *TP53*-mediated senescence program. We propose that UHRF1 overexpression is a mechanism underlying DNA hypomethylation in cancer cells and that senescence is a primary means of restricting tumorigenesis due to epigenetic disruption.

INTRODUCTION

The expression of genes that encode readers and writers of the epigenetic code are widely deregulated across cancer types (You and Jones, 2012). This contributes to the massive gene-expression changes and remodeling of the epigenetic landscape, a characteristic of many types of cancer. In particular, loss of global DNA methylation is a hallmark of cancer cells.

DNA hypomethylation contributes to oncogenesis through multiple mechanisms, including chromosomal instability (Eden et al., 2003; Karpf and Matsui, 2005), derepression of imprinted genes (Berdasco and Esteller, 2010; Jirtle, 2004; Li et al., 1993), retrotransposon activation (Gaudet et al., 2004; Howard et al., 2008; Jackson-Grusby et al., 2001; Sharif et al., 2007), and aberrant gene expression, including induction of oncogenes (Cheah et al., 1984). Many studies have documented that expression

Significance

Global DNA hypomethylation occurs in most types of cancer and can induce genomic instability and widespread changes in gene expression. UHRF1 is a key regulator of DNA methylation, and here, we show that UHRF1 overexpression causes HCC in zebrafish without any other genetic alteration, demonstrating that it is an oncogene. High UHRF1 expression causes DNA hypomethylation and *Tp53*-mediated senescence, which serves to restrict transformation of UHRF1-overexpressing cells. High *UHRF1* expression in human HCC correlates with a poor prognosis, genomic instability, *TP53* mutation, and repression of the *TP53*-mediated senescence program. We conclude that UHRF1 is an oncogene that promotes widespread DNA hypomethylation, an epigenetic hallmark of cancer cells, and that UHRF1 overexpression drives tumorigenesis when senescence is bypassed.

of the core factors required for maintenance DNA methylation—i.e., DNA methyltransferase 1 (DNMT1) and ubiquitin-like with PHD and RING finger domains 1 (UHRF1) (Babbio et al., 2012; Jin et al., 2010; Unoki et al., 2010; Wang et al., 2012)—are significantly altered across cancer types. However, whether changes in the expression of these key factors are sufficient to alter the cancer cell methylome and drive carcinogenesis is unknown. Moreover, the mechanism by which DNA methylation is lost in cancer cells is poorly understood.

The cellular response to DNA hypomethylation varies by cell type, physiological context, and degree of hypomethylation. In some cells, DNA hypomethylation induces tumor-suppressive mechanisms, including apoptosis (Anderson et al., 2009; Biniszkiewicz et al., 2002; Chen et al., 2007; Jackson-Grusby et al., 2001) or senescence (Decottignies and d'Adda di Fagagna, 2011; Fairweather et al., 1987), whereas in other cells it blocks differentiation of progenitor cells (Rai et al., 2010) or causes cancer (Gaudet et al., 2003; Yamada et al., 2005). In part, the cellular response to loss of DNA methylation is dictated by the genomic region affected: hypomethylation of gene regulatory regions, such as promoters, can derepress gene expression, whereas hypomethylation of repetitive elements can reduce heterochromatin formation and promote recombination and genomic instability.

UHRF1 plays an essential role in DNA methylation by recognizing hemimethylated DNA generated during DNA replication and then by recruiting DNMT1 to ensure faithful maintenance of DNA-methylation patterns in daughter cells (Arita et al., 2008; Avvakumov et al., 2008; Bostick et al., 2007; Hashimoto et al., 2008; Liu et al., 2013; Nishiyama et al., 2013; Sharif et al., 2007). Consequently, UHRF1 depletion results in global DNA hypomethylation (Bostick et al., 2007; Feng et al., 2010; Sharif et al., 2007; Tittle et al., 2011). Conversely, UHRF1 may also limit DNA methylation by targeting DNMT1 for ubiquitin-mediated degradation (Du et al., 2010; Qin et al., 2011) or by delocalizing DNMT1 (Sharif et al., 2007). Thus, how UHRF1 overexpression impacts the methylome is unclear.

We previously reported that *uhrf1* mutation in zebrafish blocks liver outgrowth in embryos and regeneration in adults (Sadler et al., 2007) and that depleting UHRF1 from cancer cells induces apoptosis (Tien et al., 2011). Here, we tested the hypothesis that UHRF1 overexpression would alter global DNA methylation and promote hepatocellular carcinoma (HCC).

RESULTS

High UHRF1 Expression Causes DNA Hypomethylation

UHRF1 is required for DNA methylation, as it recruits DNMT1 to hemimethylated DNA during DNA replication (Bostick et al., 2007; Feng et al., 2010; Liu et al., 2013; Nishiyama et al., 2013; Sharif et al., 2007). Paradoxically, UHRF1 also serves as an ubiquitin ligase that targets DNMT1 for degradation (Du et al., 2010; Qin et al., 2011). To determine how UHRF1 overexpression impacts DNA methylation, we generated transgenic zebrafish expressing human UHRF1 fused to GFP (*hsa.UHRF1-GFP*) under the hepatocyte-specific *fabp10* promoter (*Tg(fabp10:hsa.UHRF1-GFP)*; Chu et al., 2012).

Human and zebrafish UHRF1 are 66% identical, and the ability of human UHRF1 to rescue zebrafish embryos depleted of *Uhrf1* (V.J. and K.C.S., unpublished data; Chu et al., 2012) indicates

they are functional orthologs. Expression is first detected in hepatocytes on 3 days postfertilization (dpf) and by 5 dpf; nuclear UHRF1-GFP is easily detected at variable levels in hepatocytes (Figure S1A available online; Chu et al., 2012). We isolated an allelic series of *Tg(fabp10:hsa.UHRF1-GFP)* transgenics expressing a range of UHRF1 levels (Figures S1A and S1B; hereafter referred to *UHRF1-GFP High, Medium and Low*).

We probed genomic DNA isolated from the liver of 5 dpf larvae from each line with an antibody specific for 5-methyl cytosine (5MeC) to assess DNA methylation and found significant hypomethylation only in the liver of *UHRF1-GFP High* larvae (38% of controls; $p = 0.007$; Figures 1A and S1C). 5MeC immunofluorescence showed DNA methylation to be uniformly distributed in the nuclei of hepatocytes from control larvae that express nuclear-localized mCherry under the *fabp10* promoter (*Tg(fabp10:nls-mCherry)*; abbreviated to *nls-mCherry*). Only dim staining was detected in hepatocytes of *UHRF1-GFP High* larvae (Figure 1B). Because equivalent levels of 5MeC were detected in the liverless carcasses (Figure 1A) or cells of the fin where the transgene is not expressed (Figure 1B), we conclude that DNA hypomethylation was specific to the liver of *UHRF1-GFP High* larvae.

We hypothesized that UHRF1-induced DNA hypomethylation could be caused by mislocalization or destabilization of Dnmt1. Immunofluorescence revealed uniform Dnmt1 distribution in the nucleoplasm of *nls-mCherry* hepatocytes (Figure 1C), but in *UHRF1-GFP High* hepatocytes, it was concentrated in nuclear foci that contained UHRF1-GFP (Figure 1C). Interestingly, the range of UHRF1-GFP expression within cells of the same liver revealed that cells with high GFP had dim, punctate Dnmt1 staining, but the Dnmt1 levels and distribution pattern were similar to control hepatocytes in cells with low or no GFP-Dnmt1 levels, and the distribution pattern was similar to control hepatocytes in cells with low or no GFP (arrows, Figure 1C). Thus, UHRF1 expressed at high levels colocalizes with Dnmt1 and high UHRF1 expression redistributes Dnmt1 to intranuclear structures reminiscent of senescence-associated heterochromatin foci (Di Micco et al., 2011).

Endogenous Dnmt1 in the liver was below the levels detectable by immunoblotting (not shown), so we used a transgenic line expressing UHRF1-GFP under the inducible *hsp70I* promoter (Chu et al., 2012) to quantitatively assess the impact of UHRF1 overexpression on Dnmt1 stability at a developmental time when we could easily detect Dnmt1 levels by immunoblotting. We optimize a heat-shock protocol that maximized UHRF1-GFP expression in *Tg(hsp70I:UHRF1-GFP)* larvae (Figure 1D) and found that UHRF1-GFP overexpression reduced Dnmt1 protein by 27% compared to non-heat-shocked transgenics ($p = 0.03$; Figure 1E). Treatment with a nontoxic dose of the proteasome inhibitor, MG132, prevented the decrease in Dnmt1 induced by UHRF1 overexpression ($p = 0.01$; Figure 1E). Neither heat shock nor MG132 significantly affected Dnmt1 protein levels in nontransgenic controls (Figure 1E). Thus, both Dnmt1 delocalization and destabilization could account for DNA hypomethylation caused by UHRF1 overexpression.

DNA Hypomethylation Caused by UHRF1 Overexpression Reduces Liver Size

Uhrf1 in zebrafish is required for hepatic outgrowth and liver regeneration (Sadler et al., 2007). To determine if UHRF1

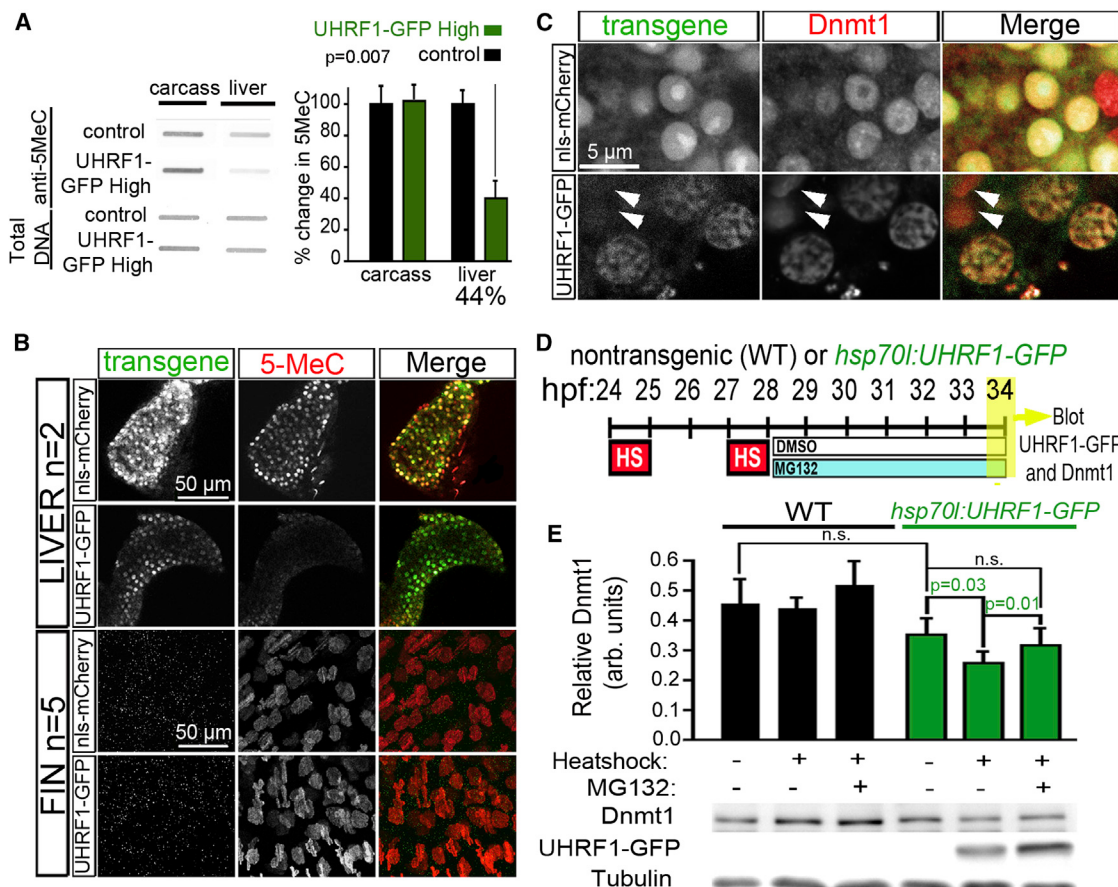


Figure 1. High UHRF1 Expression Causes Global DNA Hypomethylation

(A) 5MeC levels and total DNA stained with methylene blue were measured in 5 dpf control and *UHRF1-GFP High* livers ($n = 4$) and liverless carcasses ($n = 3$). The ratio of 5MeC to total DNA was averaged and normalized to controls. Student's t test was used to determine p values.

(B) Confocal stacks of livers (top) and fins (bottom) from 5 dpf *nls-mCherry* and *UHRF1-GFP High* larvae stained with anti-5MeC. Because a hepatocyte-specific promoter was used for transgenesis, there was no transgene expression in the fin.

(C) Dnmt1 is uniform in the hepatocyte nucleus of four dpf *nls-mCherry* larvae but is found in GFP-containing punctae in *UHRF1-GFP High* hepatocytes. Arrows point to cells that do not express GFP and have Dnmt1 distribution pattern similar to controls.

(D) *Tg(hsp70l:UHRF1-EGFP)* and nontransgenic controls were heat shocked at 37°C for 1 hr at 24 and 27 hpf, treated with 10 µM MG132 or DMSO at 28 hpf, and collected at 34 hpf for immunoblotting.

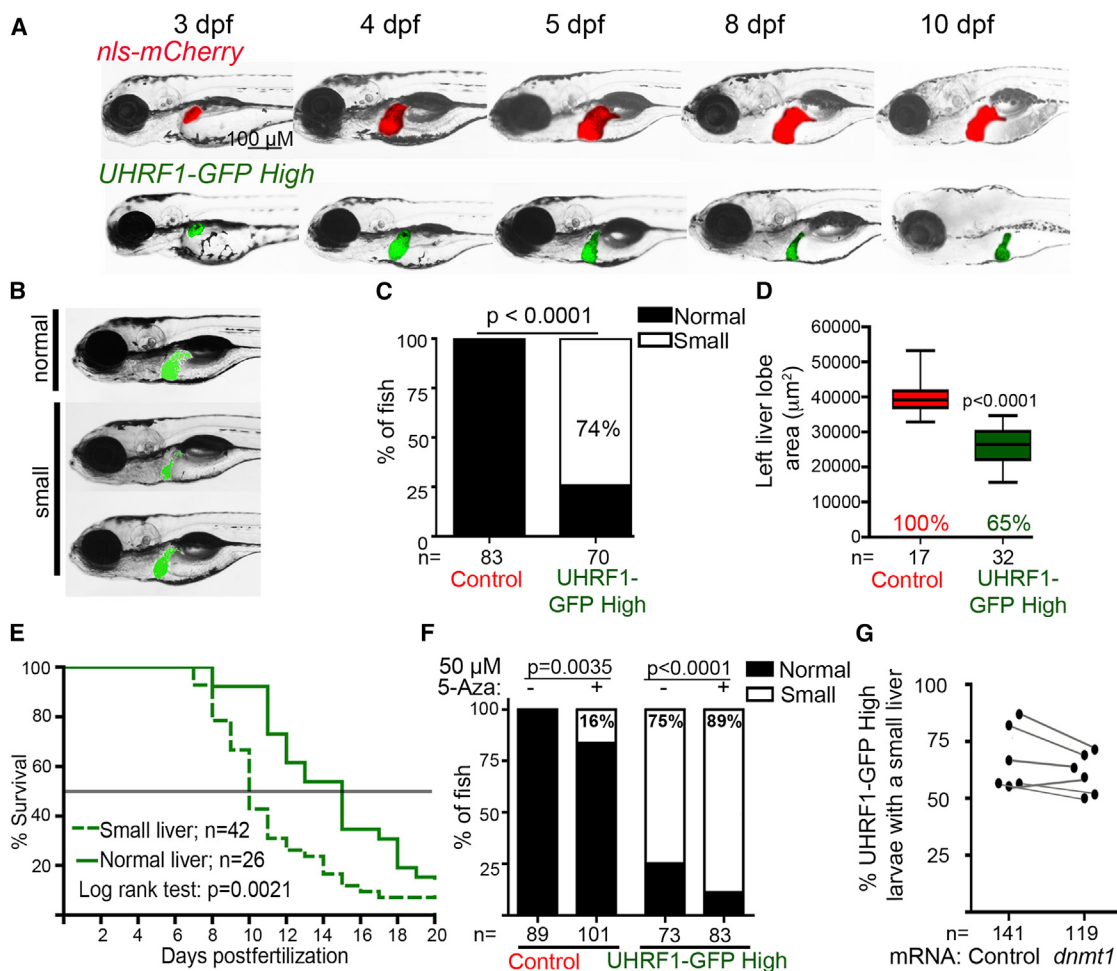
(E) Dnmt1 levels normalized to tubulin were averaged from six experiments. Student's t test was used to determine p values; n.s., not significant; error bars represent SD.

See also Figure S1.

overexpression in hepatocytes affected hepatic outgrowth, we assessed liver size in fish from all transgenic lines (Figures 2A–2C and S2A). Low and medium expressing lines had no gross changes in liver size (Figure S2A), but 74% of *UHRF1-GFP High* larvae on 5 dpf had small livers (Figure 2C), with the median area of the left liver lobe reduced by 35% compared to controls ($p < 0.001$; Figures 2D and S2A), without reduction of total fish size (Figure S2B).

Larvae with small livers appeared sick (see 10 dpf larvae in Figure 2A), and only 20% of *UHRF1-GFP High* fish survived to 20 dpf (Figures S2C and 2E). Moreover, *UHRF1-GFP High* larvae with the “microliver” phenotype on 5 dpf had significantly higher mortality by 10 dpf (67%) than those that started with a normal-sized liver (7%; Figure 2E). Thus, high UHRF1 expression in hepatocytes causes DNA hypomethylation, microliver, and larval death.

We next investigated the relationship between DNA hypomethylation and the microliver phenotype by asking whether further reducing DNA methylation could enhance this phenotype or restoring Dnmt1 could suppress it. We previously reported that exposing embryos to 50 µM of the Dnmt1 inhibitor, 5-azacytidine (5-Aza) from 0 to 5 dpf caused a profoundly small liver and DNA hypomethylation (Mudbhary and Sadler, 2011). By restricting the 5-Aza exposure time to 2.5–5 dpf, we reduced DNA methylation in the liver of control larvae by 40% (Figure S1C), which induced a moderately small liver in 16% of larvae ($p = 0.0035$; Figure 2F). This same treatment of *UHRF1-GFP High* larvae significantly increased the percent with small livers ($p < 0.0001$; Figure 2F). Whereas this could be attributed to DNA damage caused by 5-Aza, our finding that injecting *UHRF1-GFP High* embryos with mRNA-encoding Dnmt1 modestly suppressed

**Figure 2. UHRF1-Induced Hypomethylation Reduces Liver Size**

- (A) Individual larvae were imaged daily from 3–10 dpf.
- (B) Five dpf UHRF1-GFP High larvae display a range of liver sizes scored as “normal” or “small”.
- (C) Three clutches were scored according to criteria in (B); n, number of larvae. Fisher’s exact test was used to determine p value.
- (D) The area of the left liver lobe was measured in 5 dpf fish from two clutches. Boxes represent 75th and 25th percentile, horizontal line is the median, and whiskers mark lowest and highest values. Student’s t test was used to determine p value.
- (E) UHRF1-GFP High larvae were sorted by liver size on 5 dpf and tracked daily for survival to 20 dpf. Data are pooled from three clutches.
- (F) UHRF1-GFP High and control larvae were treated with 50 μM 5-Aza from 2.5–5 dpf and scored for liver size in six clutches. Fisher’s exact test was used to determine p values.
- (G) UHRF1-GFP High embryos were injected with mRNA encoding *dnmt1* or *Mpi* before 1 hpf. The percent of fish with a normal liver size was scored at 5 dpf in six clutches.

See also Figure S2.

the percent of fish with a small liver (Figure 2G) and increased the average size of the left liver lobe by 10%–15% (Figure S2D) suggests that hypomethylation, at least in part, contributes to the small-liver phenotype of UHRF1-GFP High larvae.

UHRF1 Overexpression Triggers Tp53-Mediated Senescence

DNA hypomethylation can induce apoptosis, but we found no TUNEL-positive cells on 5 dpf in UHRF1-GFP High livers (Figure S3A). However, senescence-associated β -galactosidase (SA- β -gal) staining was detected throughout the liver of most UHRF1-GFP High 5 dpf larvae (n = 93; Figures 3A and 3B), but not other transgenic lines (Figure S3B). Additionally, the DNA

in control hepatocytes was evenly distributed throughout the uniformly sized nuclei compared to the large nuclei where DNA resembled senescence-associated heterochromatic foci (inset, Figure 3C). Strikingly, the largest hepatocyte nuclei also had the brightest GFP (Figure 3C), suggesting the effect of UHRF1 overexpression cell autonomously affected nuclear morphology.

Senescent cells do not divide, and we found significantly less bromodeoxyuridine (BrdU) incorporation in the liver of 5 dpf UHRF1-GFP High larvae compared to controls (p < 0.0001; Figure 3D). Interestingly, in *nls-mCherry* larvae, most BrdU incorporation was detected in hepatocytes that express *nls-mCherry*, but the only BrdU-positive cells in UHRF1-GFP High larvae were negative for GFP (see inset in Figure 3D). RNA sequencing

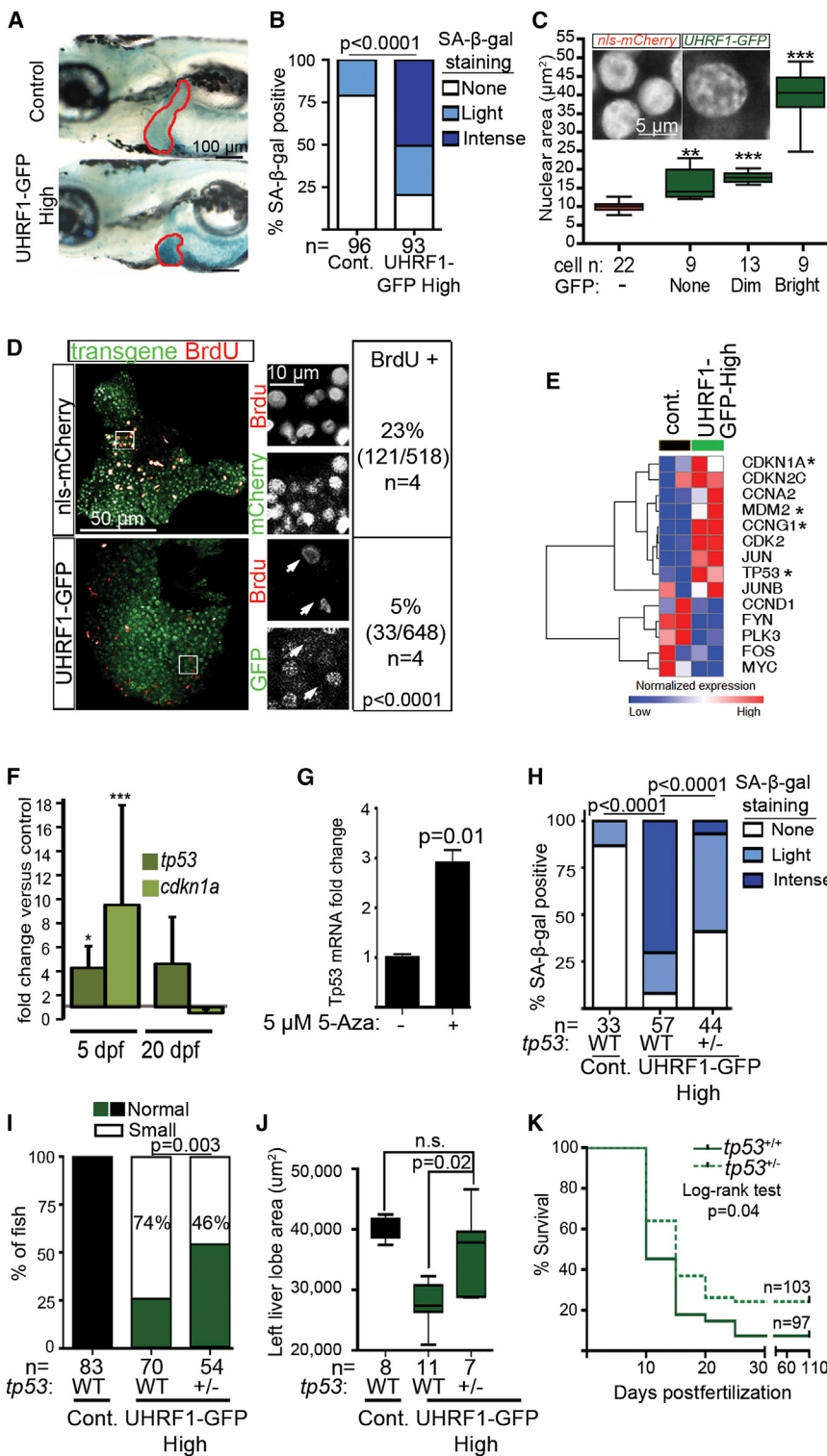


Figure 3. UHRF1 Overexpression in Hepatocytes Induces Tp53-Mediated Senescence

(A) Intense senescence-associated β -galactosidase (SA- β -gal) staining was detected in the liver (outlined) of 5 dpf *UHRF1-GFP High* larvae compared to light or no staining in controls.

(B) Five dpf fish from five clutches were scored for hepatic SA- β -gal staining. ***p < 0.0001 by Fisher's exact test.

(C) Nuclear size was measured in hepatocytes of a single control or *UHRF1-GFP High* 5 dpf liver, and cells were stratified according to GFP expression. Inset shows confocal stack of the DNA organized into foci. **p < 0.01 and ***p < 0.0001, compared to nuclear size in *nls-mCherry* larvae.

(D) BrdU-positive cells and the total number of transgene-expressing hepatocytes in *nls-mCherry* and *UHRF1-GFP High* 5 dpf larvae (bottom) 5 dpf larvae. A Fisher's exact test was used to calculate p value. In *nls-mCherry* larvae, most BrdU-positive cells also express the transgene, whereas the BrdU-positive cells in *UHRF1-GFP High* livers did not express GFP (white arrows in magnified regions, which are marked by the white box).

(E) Heatmap of log2 values from RNA-seq shows cell-cycle regulators are down and Tp53 target genes (marked by *) are up in *UHRF1-GFP High* 5 dpf livers.

(F) *tp53* and *cdkn1a* mRNA expression were induced on 5 dpf and downregulated on 20 dpf in *UHRF1-GFP High* livers. *p = 0.05; ***p = 0.001 calculated by one sample Student's t test. Error bars represent SD.

(G) 5-Aza induces *Tp53* expression in primary mouse hepatocytes. Student's t test was used to determine p value with SD indicated by the error bars across three replicates.

(H–K) *tp53^{+/−}* in *UHRF1-GFP High* larvae significantly reduced SA- β -gal staining in the liver (two clutches) (H), and increased the percent of larvae with normal liver size (I), the area of the left liver lobe (J), and survival at 5 dpf (K). p values were calculated with a Fisher's test with Freeman-Halton extension (H), Fisher's exact test (I), and Student's t test. Boxes represent 75th and 25th percentile, horizontal line is the median, and whiskers mark lowest and highest values (J). See also Figure S3.

(RNA-seq) analysis of liver samples from 5 dpf revealed down-regulation of some proproliferative genes (*ccnd1* and *myc*) (Figure 3E), lending further support to the conclusion that senescence is the primary response to high UHRF overexpression in hepatocytes during hepatic outgrowth.

TP53 is a key mediator of senescence caused by DNA damage and oncogenic stress (Di Micco et al., 2011; McDuff and Turner, 2011; Ventura et al., 2007; Xue et al., 2007). RNA-seq (Figure 3E) and quantitative PCR (qPCR) analysis (Figure 3F) show that *tp53* and its target genes, especially *cdkn1a*, are significantly induced in the liver of 5 dpf *UHRF1-GFP High* larvae but then return to baseline by 20 dpf (Figure 3F). 5-Aza treatment of primary mouse hepatocytes induced *Tp53* expression (Figure 3G), similar to the effects of 5-Aza treatment or Dnmt1 depletion in other mammalian cell types (Jackson-Grusby et al., 2001;

Karpf et al., 2001) and in zebrafish embryos (V.J. and K.C.S., unpublished data; not shown). However, because significant alteration in methylation of the *tp53* promoter was not detected in these models (not shown), we hypothesize that DNA methylation does not directly regulate *Tp53* expression. Instead, DNA hypomethylation may induce *tp53* by an indirect mechanism, such as increased DNA damage or genomic instability.

A direct role for Tp53 in the phenotypes induced by UHRF1 overexpression was demonstrated by removing one copy of *tp53*. This reduced the incidence and intensity of SA- β -gal staining in the liver (Figure 3H), increased liver size (Figures 3I and 3J), and reduced mortality (Figure 3K) of *UHRF1-GFP High* fish. We thus propose a model whereby high UHRF1 causes DNA hypomethylation, induces Tp53-mediated senescence, which prevents expansion of the hepatic bud, resulting in hepatic insufficiency and larval death.

UHRF1 Overexpression Induces Liver Cancer in Zebrafish

To determine if UHRF1 overexpression was sufficient to cause HCC, 281 control and *UHRF1-GFP* transgenics were collected between 5 and 300 dpf, serial sectioned, and analyzed for atypical cells, dysplastic foci, and HCC using histological criteria devised by two expert pathologists (R.T.B. and M.I.F.), which included disrupted tissue architecture, cell size, shape, nuclear structure, and the presence of mitotic figures (Figures S4A and S4B). Evidence of increased hepatocyte proliferation was detected in all UHRF1-overexpressing lines on 20 and 40 dpf (Figure S4C), but this was insufficient to cause HCC, as *UHRF1-GFP Low* fish were tumor free at all time points (Table 1). In contrast, *UHRF1-GFP High* fish developed atypical hepatocytes as early as 5 dpf, with an 8% incidence of dysplastic foci and 46% incidence of HCC by 15 dpf. On 20 dpf, 76% of fish had HCC (Figures 4A and 4B; Table 1). *UHRF1-GFP Medium* fish also developed atypical hepatocytes and dysplastic foci at young ages, and one large HCC was detected in a 60 dpf fish (Table 1). In a classical transformation assay using NIH 3T3 cells, UHRF1 cooperated with RAS to promote growth on soft agar (Figure 4C). These conclusively demonstrate that UHRF1 is an oncogene.

We found that *UHRF1-GFP High* larvae older than 8 dpf had a lower incidence and intensity of hepatic SA- β -gal staining (Figure 4D). Interestingly, in many of these fish, intense staining was distributed in a punctate pattern. By 20 dpf, 75% of fish had either punctate or no staining (Figure 4D), which is a striking correlation with the 70% incidence of HCC at this time point. This was mirrored by increased proliferation of liver cells, detected by increased BrdU incorporation in *UHRF1-GFP High* livers (22% versus 4% in controls) at 11 dpf ($p < 0.001$; Figure 4E), and higher PCNA staining on 20 and 40 dpf in all lines (Figure S4C). Loss of senescence was not attributed to re-establishment of DNA methylation or transgene silencing, as reduced 5MeC staining persisted in tumor cells (Figure S4D) and transgene expression was detectable in all 20 dpf fish (Figures S4E and S4F), albeit reduced from levels detected in 5 dpf livers.

We asked whether Tp53 epistatically interacted with UHRF1 overexpression to contribute to HCC by removing one copy of *tp53* (Berghmans et al., 2005). The liver appeared normal in 13 *tp53^{+/−}* fish without transgene expression (not shown), but in *UHRF1-GFP High* fish, tumor incidence on 15 dpf increased

from 50% in wild-type (WT) to 87% in *tp53^{+/−}* fish (Figure 4B). Interestingly, in a single *UHRF1-GFP High*; *tp53^{+/−}*, 15 dpf fish, we found a tumor with immature cells resembling a cholangiocarcinoma. Thus, *tp53* functions to suppress tumor formation and may alter the spectrum of tumors caused by UHRF1 overexpression.

UHRF1 Is Upregulated in Human HCC

We next investigated the relevance of UHRF1 expression in human HCC. We assessed UHRF1 expression by qPCR in 16 normal liver samples and in two cohorts of patients with dysplastic nodules or HCC: the first cohort of 58 patients had hepatitis C infection (HCV) (Figure 5A; Wurmbach et al., 2007), and the second cohort of 69 patients had hepatitis B virus, alcohol, and other etiologies (Figure S5A; Villanueva et al., 2008). Additional publicly available transcriptome data sets from three other cohorts of HCCs (Figure S5B) and from lung, gastric, colorectal, and breast cancer (Figure S5C) were also analyzed. All showed elevated *UHRF1* in tumors, with expression elevated >2-fold compared to controls in 17/18 dysplastic foci and 104/109 HCCs (Figures 5A and S5A). An average of 20- and 46-fold overexpression of *UHRF1* was detected in advanced and very advanced HCCs. UHRF1 protein was barely detectable in five normal liver samples but highly expressed in 38/52 (73%) of the tumors analyzed for *UHRF1* mRNA in Figure 5A ($p < 0.003$; Figure 5B). Thus, *UHRF1* is overexpressed in HCCs of diverse etiologies as well as in other tumor types, and high *UHRF1* expression is significantly associated with the most advanced tumors.

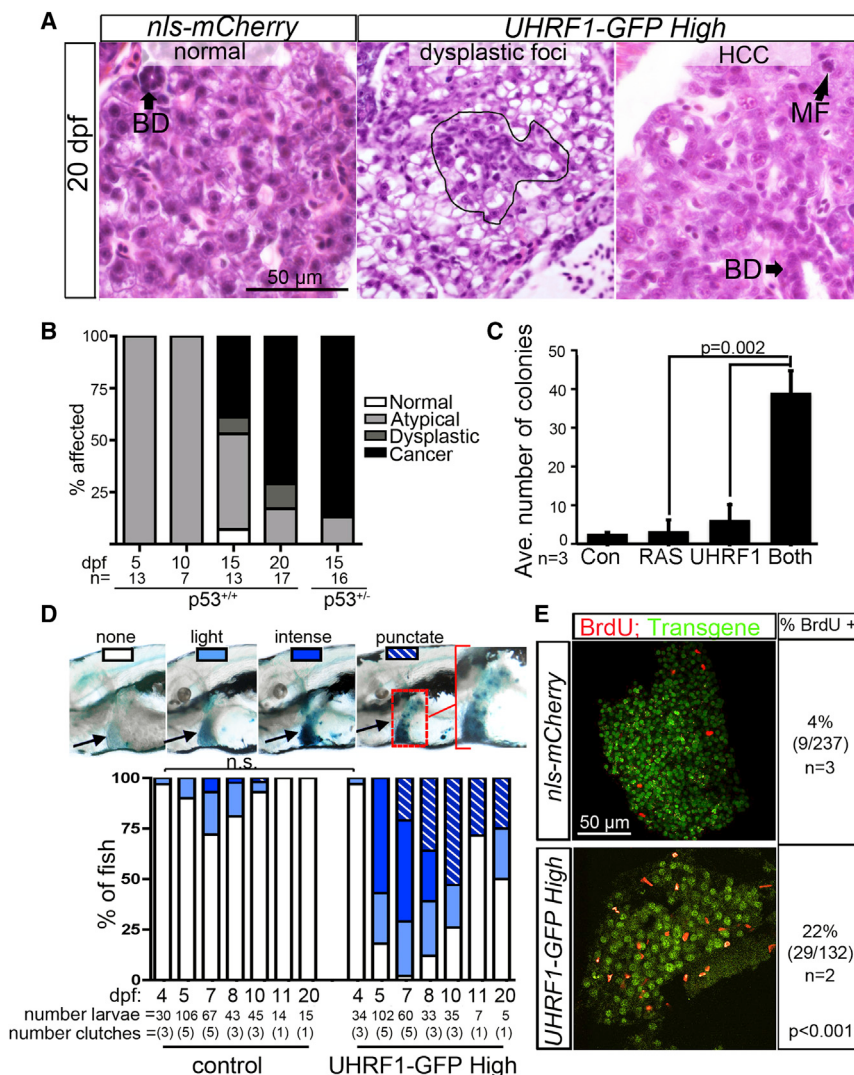
Targeting UHRF1 in liver cancer cells (HepG2) using small interfering RNA (siRNA) induced PARP cleavage (Figure 5C) and other markers of apoptosis (not shown), similar to results obtained using another HCC cell line (Hep3B; not shown) and colon cancer cells (Tien et al., 2011). Thus, blocking UHRF1 in cancers with high UHRF1 expression could be an effective means to induce tumor cell death.

Of the 109 HCCs analyzed for *UHRF1* expression by qPCR, 71 had multiple clinical and genomics parameters available (Chiang et al., 2008). These were rank-ordered based on *UHRF1* expression determined by qPCR (Figure 6A). Tumors with expression above and equal to or below the median log2-fold change value of 3.64 were designated as “high” ($n = 35$) and “low” ($n = 36$), respectively (Figure 6A). High-*UHRF1*-expressing tumors were associated with signs of poor clinical outcome: 80% had microvascular invasion (Figure 5D) and significantly higher alpha-fetoprotein (AFP) levels (Figure 5E), although AFP levels alone did not cooperate with UHRF1 to predict survival (data not shown). Importantly, high *UHRF1* expression significantly correlated with early (<2 years; Figure 5F), but not late (Figure 5G), tumor recurrence and was inversely correlated with survival (Figure 5H). This suggests that high *UHRF1* expression predicted recurrence of the primary tumor, causing decreased survival (Villanueva et al., 2011). Molecular signatures of aggressive HCC tumors compiled from several previous studies (Table S1) were concordantly and significantly enriched in high-*UHRF1*-expressing tumors (Figure 6A). Moreover, high-*UHRF1*-expressing tumors were distinguished by induction of pathways that drive the cell cycle, DNA replication, and repair (Figure S6A; Tables S2 and S3). *UHRF1* overexpression also significantly

Table 1. HCC Onset and Incidence in *Tg(fabp10:nls-mCherry*) and *Tg(fabp10:UHRF1-GFP*) Zebrafish

Transgene	dpf	5	10	15	20	25	30	40	50	60	90	180	300	Total n = 281	CI
<i>nls-mCherry</i>	normal	100%	100%	100%	100%			100%	100%	100%	100%	100%	100%	65	100%
	atypical cells	0%	0%	0%	0%			0%	0%	0%	0%	0%	0%	0	0%
	dysplastic foci	0%	0%	0%	0%			0%	0%	0%	0%	0%	0%	0	0%
	tumor	0%	0%	0%	0%			0%	0%	0%	0%	0%	0%	0	0%
	n =	8	8	8	11	nd	nd	5	5	5	5	5	5	65	
<i>UHRF1-GFP Low</i>	normal	100%	100%	100%	100%			100%			100%	100%	100%	60	100%
	atypical cells	0%	0%	0%	0%			0%			0%	0%	0%	0	0%
	dysplastic foci	0%	0%	0%	0%			0%			0%	0%	0%	0	0%
	tumor	0%	0%	0%	0%			0%			0%	0%	0%	0	0%
	n =	7	9	10	12	nd	nd	4	nd	nd	6	6	6	60	
<i>UHRF1-GFP Medium</i>	normal	90% (9)	100% (11)	50% (3)	28% (4)	66% (4)	80% (4)	50% (4)	50% (5)	81% (13)				57	66%
	atypical cells	10% (1)	0%	50% (3)	57% (8)	33% (2)	20% (1)	50% (4)	20% (2)	44% (7)				28	32%
	dysplastic foci	0%	0%	0%	7% (1)	0%	0%	25% (2)	30% (3)	0%				6	7%
	tumor	0%	0%	0%	0%	0%	0%	0%	0%	6% (1)				1	1%
	n =	10	11	6	14	6	5	8	10	16				86	
<i>UHRF1-GFP High</i>	normal	0%	0%	7% (1)	0%			0%						1	2%
	atypical cells	100% (13)	100% (7)	46% (6)	17% (3)			75% (3)						36	61%
	dysplastic foci	0%	0%	8% (1)	12% (2)			25% (1)						4	7%
	tumor	0%	0%	46% (6)	76% (13)			0%						18	30%
	n =	13	7	13	17			4						54	
<i>UHRF1-GFP High/ p53^{+/-}</i>	normal		0%											0	0%
	atypical cells		13% (2)											2	13%
	dysplastic foci		0%											0	0%
	tumor		88% (14)											14	88%
	n =		16											16	

The incidence (percent) and absolute number of fish (parentheses) with cancer-relevant histological phenotypes were scored in a total of 281 fish from four transgenic lines. The total n for each time point is indicated. Some fish were diagnosed with more than one lesion. nd, not done; CI, cumulative incidence.

**Figure 4. UHRF1 Is an Oncogene**

(A) Atypical cells, dysplastic foci (outlined), and HCC are apparent in hematoxylin and eosin-stained *UHRF1-GFP High* livers. BD, bile duct; MF, mitotic figure.

(B) Incidence of normal and atypical hepatocytes, dysplastic foci, and cancer in the liver of *UHRF1-GFP High* fish on WT or *tp53^{+/−}* background.

(C) NIH 3T3 cell growth in soft agar is enhanced when UHRF1 overexpression is combined with RAS (n = 3). The p value was calculated by Student's t test, and error bars represent the SD.

(D) Hepatic SA- β -gal-staining patterns in *UHRF1-GFP High* larvae change as fish age. Images of 8 dpf larvae illustrate the SA- β -gal-staining patterns that were scored in the time course shown in the graph. A significant increase in the number of *UHRF1-GFP High* fish with intense or punctate SA- β -gal compared to controls at all time points (p < 0.01 by Fisher's exact test) except at 4 dpf; n.s., not significant.

(E) BrdU incorporation in the liver on 11 dpf is five times higher in *UHRF1-GFP High* fish than in controls. Total number of cells counted is indicated with n = number of clutches assessed. Fisher's exact test was used to calculate p value. See also Figure S4.

correlated with advanced-stage prostate cancer, but not lung or colon (Figures S5D–S5G).

High UHRF1 Expression Delineates a Subclass of HCCs that Have Downregulated TP53-Mediated Senescence

Our zebrafish studies demonstrated that bypass of Tp53-induced senescence is required for UHRF1 to act as an oncogene. Our analysis of human HCCs indicates that a similar paradigm occurs in these samples. First, inactivating mutations in *TP53* significantly correlated with high *UHRF1* expression (Figure 6A). Second, many of the core enriched genes high-UHRF1-expressing tumors are regulated by TP53 in senescent fibroblasts (Table S4; Tang et al., 2007), and high-UHRF1-expressing tumors downregulated the gene expression signature associated with TP53-induced senescence in fibroblasts (Table S5; Figure S6B; Tang et al., 2007) and in hepatic stellate cells (Table S6; Figure S6C; Lujambio et al., 2013). Fourth, significant correlation between *UHRF1* overexpression, *TP53* mutation, and genome integrity in human HCCs indicates that these pathways act together, where high *UHRF1* expression (Figures

6B and 6C) and *TP53* mutation (Figure 6D) are independently correlated with chromosomal loss, but tumors that have both features display even more chromosomal loss (Figure 6D). Finally, *UHRF1* expression was significantly higher in tumors with *TP53* mutation (Figure 6E). *UHRF1* overexpression did not correlate with copy-number variation at the *UHRF1* locus (Figure S6D) suggesting that a different mechanism drives UHRF1 overexpression.

Genome-wide DNA hypomethylation is found in most HCCs (Calvisi et al., 2007), and this rendered it difficult to correlate methylome changes with *UHRF1* expression. However, *DNMT1* expression was directly correlated with *UHRF1* expression in HCC samples (Figure 6F). This may be a consequence of the high proliferation rate in these tumors or an induction of the methylation machinery to compensate for hypomethylation. Together, these data indicate that high UHRF1 expression in HCC defines a subset of aggressive tumors that have inactivated the TP53-induced senescence program, suggesting that, in humans, as observed in zebrafish, TP53 acts as a tumor suppressor to restrict the oncogenic potential of UHRF1-overexpressing cells.

DISCUSSION

We show that UHRF1 overexpression is sufficient to cause two oncogene-associated phenotypes: senescence and cancer. This defines UHRF1 as an epigenetic regulator that causes cancer upon overexpression, and it is thus an oncogene. We

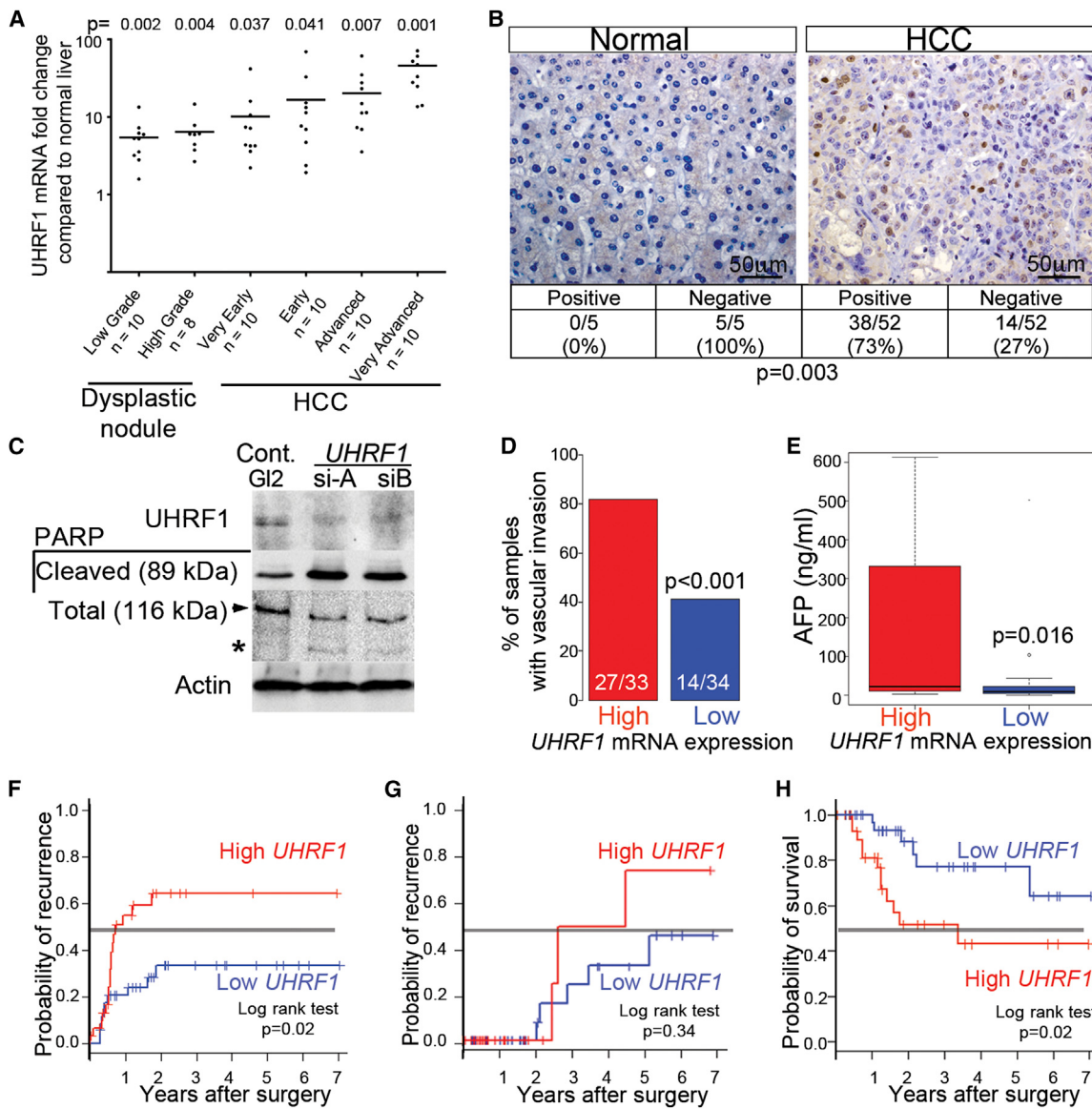


Figure 5. UHRF1 mRNA and Protein Are Overexpressed in HCC

(A) UHRF1 detected by qRT-PCR in 18 preneoplastic lesions and 40 HCCs from hepatitis C virus (HCV)-infected patients compared to expression in nine normal livers. Horizontal line indicates median.

(B) Immunohistochemistry for UHRF1 protein (brown) was evaluated in 52 of the same HCCs examined in (A) plus five normal liver samples. Fisher's exact test was used to calculate p value. Seventy-one of the HCV-associated HCCs analyzed by qPCR were grouped into high ($n = 35$) and low ($n = 36$) UHRF1-expressing tumors based on the median log2-fold change of 3.64.

(C) HepG2 cells transfected with control siRNA (GL2) or two different siRNAs targeting *UHRF1* described in Tien et al. (2011) were blotted for UHRF1 and cleaved and total PARP (arrow indicates full length; * indicates cleaved protein).

(D–H) Vascular invasion (33 high and 34 low tumors; four missing values) (D), serum AFP (29 UHRF1-high and 29 low tumors; 13 missing values) (E), early (<2 years) (F) and late (>2 years; 32 UHRF1-high and 35 low tumors; four missing values) (G) tumor recurrence, and overall survival after surgery (32 high and 35 low tumors; four missing values) (H) were stratified according to *UHRF1* expression. Continuous and categorical variables were assessed by Wilcoxon rank-sum test and Fisher's exact test, respectively. Clinical outcome difference was evaluated by log rank test. In box and whisker plots, boxes represent the 75th and 25th percentiles, the whiskers represent the most extreme data points within interquartile range \times 1.5, and the horizontal bar represents the median.

See also Figure S5.

hypothesize that UHRF1 overexpression is one mechanism by which cancer genomes can become hypomethylated, either via UHRF1-mediated Dnmt1 ubiquitination and degradation (Du et al., 2010; Qin et al., 2011) or by redistribution and/or sequestration of Dnmt1 away from DNA. Excess UHRF1 might

also sequester the DNMT1-deubiquitinating enzyme, USP7 (Qin et al., 2011), to further promote DNMT1 ubiquitination and degradation.

The precise mechanism by which DNA hypomethylation causes cancer remains elusive. Both apoptosis and senescence

serve to limit the propagation of cells with aberrant DNA methylation (Decottignies and d'Adda di Fagagna, 2011; Fairweather et al., 1987); however, once epigenetically altered cells escape these tumor-suppressive mechanisms, they likely accumulate genetic lesions that predispose to cancer. Indeed, chromosomal instability and mitotic catastrophe occur following DNMT1 depletion (Chen et al., 2007; Karpf and Matsui, 2005; Weber and Schübeler, 2007), and transposons, which are heavily methylated in normal cells, could become activated and cause genomic instability upon UHRF1-induced DNA hypomethylation. Additionally, hypomethylated DNA is more likely to assume an open chromatin conformation, which may promote oncogene expression, although this possibility has not been fully evaluated. Whereas the oncogenic role of UHRF1 could also be mediated by the impact of UHRF1 on other epigenetic marks or on DNA replication (Taylor et al., 2013), our data combined with findings from others (Eden et al., 2003; Gaudet et al., 2003) suggest that DNA hypomethylation is a likely mechanism driving UHRF1-mediated transformation.

Our working model (Figure 7) proposes that UHRF1 overexpression causes DNA hypomethylation by reducing Dnmt1 levels and its access to hemimethylated DNA. Tp53 is then induced in response to either genomic instability or some other mechanism, causing hepatocyte senescence, which prevents hepatic expansion and results in larval death from hepatic insufficiency. We propose that Tp53 inactivation and senescence bypass by an as of yet unknown mechanism and allow for unhindered cell proliferation and malignant transformation. How this tumor-suppressive mechanism is overcome remains a central, unanswered question in cancer biology.

Studies in a mouse liver cancer model show that Tp53 reactivation causes senescence, and these cells are then cleared by the immune system (Xue et al., 2007) and the liver is then repopulated with senescence-resistant tumor-forming cells. Our finding that senescence decreases and BrdU incorporation increases in *UHRF1-GFP High* livers over time suggests a similar process at play. Moreover, BrdU incorporation in primarily GFP-negative cells suggests the expansion of either immune cells or immature hepatic progenitors in response to senescent hepatocytes. The finding of a cholangiocarcinoma in a *UHRF1-GFP High/p53^{-/-}* fish may indicate a bipotential progenitor cell as the tumor-forming cell in this model. Additionally, our data indicate that there is a threshold effect of UHRF1 expression, in which the highest expressing cells undergo senescence and neighboring hepatocytes expressing UHRF1-GFP at levels below those detectable via microscopy undergo unhindered expansion.

HCC is the third cause of cancer-related deaths globally (Llovet et al., 2003), yet curative therapies are limited, with sorafenib as the only systemic therapy available for advanced cases (Llovet et al., 2008). Thus, there is an urgent and unmet need for novel therapies. HCC, like other cancers, is characterized by global DNA hypomethylation (Calvisi et al., 2007; Pogribny and Rusyn, 2014; Tischoff and Tannapfe, 2008), and high UHRF1 expression could be the cause. Our finding that UHRF1 depletion in HCC and other types of cancer cells causes apoptosis (Tien et al., 2011) presents UHRF1 as an attractive target for inducing cancer cell death induced by massive epigenetic changes incompatible with cell survival or by resetting

the cancer cell methylome to reinstate the expression of genes that block cell proliferation.

EXPERIMENTAL PROCEDURES

Zebrafish Maintenance and Generation of Transgenics

Zebrafish were maintained on a 14:10 hr light:dark cycle at 28°C. mRNA-encoding zebrafish Dnmt1 (Rai et al., 2006) or mannose phosphate isomerase (Mpi) (Chu et al., 2013) as a control was injected into embryos just after fertilization.

Tg(fabp10:nls-mCherry) fish expressing nls-mCherry exclusively in hepatocytes were generated using Gateway cloning (Invitrogen) to produce vectors with *tol2* transposon sites (Kwan et al., 2007). *Tg(hsp70l:hsa.UHRF1-GFP)* and *Tg(fabp10:hsa.UHRF1-GFP)* were described in Chu et al. (2012). The high, medium, and low expressing alleles are listed at <http://www.ZFIN.org> with superscripts *mss1a*, *mss1b*, and *mss1c*, respectively. Transgenics were outcrossed to Tab14 (WT) or *tp53^{-/-}* fish (Berghmans et al., 2005).

Tg(hsp70l:UHRF1-GFP) embryos were heat shocked at 37°C for 1 hr at 24 and 27 hr postfertilization (hpf). At 28 hpf, embryos were sorted visually for GFP expression and incubated with either 10 μM MG132 or DMSO and collected for immunoblotting at 34 hpf. 5-Aza (50 μM) was added to larvae from 2.5 to 5 dpf. The Mount Sinai Institutional Animal Care and Use Committee approved all protocols. Nomenclature guidelines for the species under discussion were followed, and when no species are specified, human nomenclature was used.

Gene-Expression Analysis

RNA was isolated from a pool of at least ten livers from 5 dpf fish and from one to five livers from 20 dpf fish using the RNeasy mini-kit (QIAGEN). cDNA was prepared by polyA priming using qScript SuperMix (Quanta). Quantitative RT-PCR (qRT-PCR) analysis was performed in the Light Cycler 480 (Roche) using gene-specific primers (see *Supplemental Information*) and PerfeCTa SYBRGreen FastMix (Quanta). Ct values from triplicate reactions were averaged and $2^{-\Delta \Delta Ct}$ was used to calculate expression, with *rpp0* and cyclophilin A used as reference genes of zebrafish and mouse samples, respectively.

RNA-seq analysis was carried out on RNA from pools of 50 livers dissected from two clutches of 5 dpf *UHRF1-GFP High* and *nls-mCherry* larvae, described in *Supplemental Information*.

Histology

Fish younger than 20 dpf were fixed overnight at 4°C in 4% paraformaldehyde (PFA), and older fish were fixed for 2–5 days at room temperature in Bouin's fixative. Four micromolar serial sections of paraffin-embedded fish were stained with hematoxylin and eosin as described (Imrie and Sadler, 2010) and imaged on an Olympus BX41 clinical microscope equipped with a Nikon DS-Ri1 digital camera. Histological criteria used for scoring tumors are described in Figures S4A and S4B.

Immunoblotting

Lysates prepared from 15 embryos dissolved in 150 μl protein lysis buffer were homogenized by sonication. One embryo equivalent was loaded per lane of an 8% or 12% SDS gel, transferred to nitrocellulose, and blotted. HepG2 cell lysates were prepared as described (Tien et al., 2011).

Antibodies

Antibodies recognizing DNMT1 (1:1,000 for blotting; 1:10 for immunofluorescence; Santa Cruz Biotechnology), UHRF1 (immunoblotting: 1:1,000; BD Biosciences; immunohistochemistry: 1:50; ab57083; Abcam), tubulin (1:5,000; Developmental Studies Hybridoma Bank), p89 PARP and total PARP (1:1,000; Cell Signaling Technology), B-actin (1:2,000; Sigma), 5MeC (1:500; Eurogentec), BrdU (1:200; BD Biosciences), and anti-rabbit or mouse conjugated to Alexa 555 or Alexa 488 (1:100; Invitrogen) were diluted in 10% fetal bovine serum (FBS) or 2% BSA in 1% Triton in PBS (PBST).

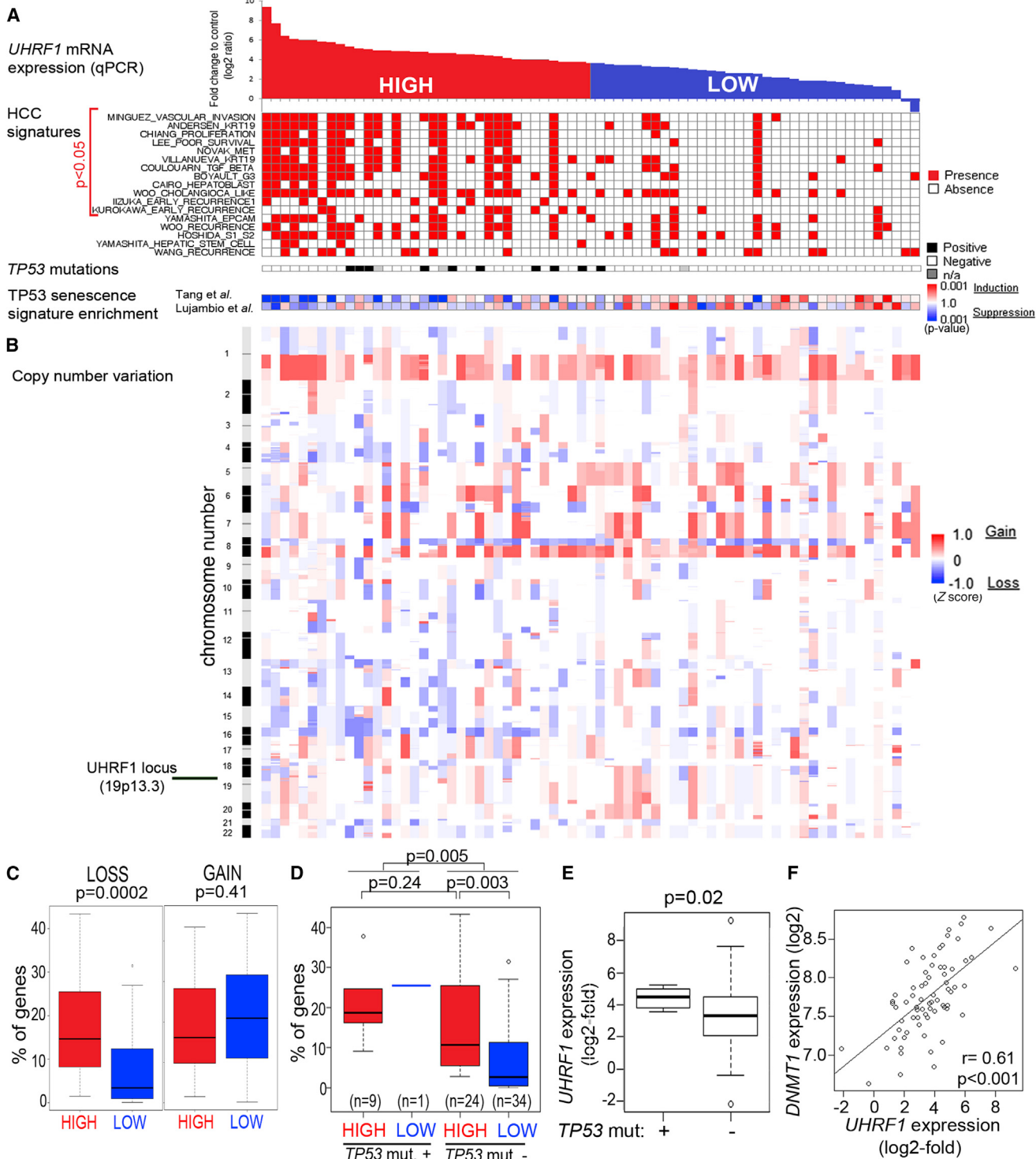


Figure 6. High *UHRF1* Expression Defines a Subclass of Tumors with Inactivated tp53, Repression of Senescence, and Chromosomal Instability

(A) The 71 human HCC tumors analyzed in Figures 5C–5G were rank-ordered according to *UHRF1* expression by qPCR and classified as high (<median, red; n = 35) or low (\geq median, blue; n = 36). The presences of aggressive human HCC gene signatures from published studies and of TP53-inactivating mutations are indicated by red and black boxes, respectively. TP53-mediated senescence gene signatures (Lujambio et al., 2013; Tang et al., 2007) are displayed as a range from repressed (blue) to activated (red).

(B) Genome-wide profile of DNA copy number variation was obtained from Gene Expression Omnibus gene set GSE9829.

(C) Proportion of genes with DNA copy number loss and gain in tumors according to *UHRF1* expression.

(legend continued on next page)

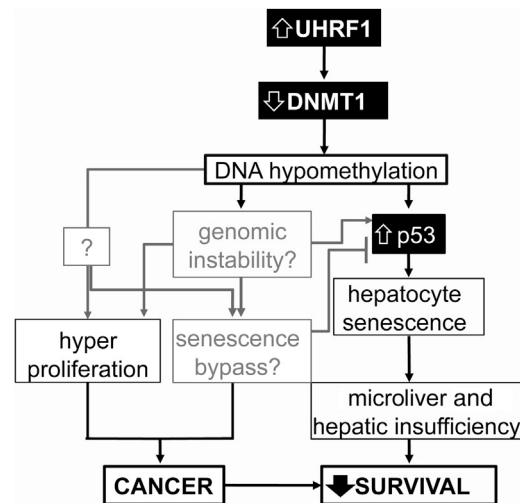


Figure 7. Model of the Relationship between UHRF1 Overexpression, DNA Hypomethylation, Tp53-Mediated Senescence, Cancer, and Survival

Factors investigated in this study are in solid black boxes with black lines indicating the correlations demonstrated in this work and gray lines indicating relationships that are speculative. Senescence reduces liver size and function and reduces larval survival, whereas cancer occurs when senescence is bypassed and also reduces survival.

Zebrafish Staining

Larvae fixed in 4% PFA were washed in PBST and stained using the Senescence β -Galactosidase Staining Kit (Cell Signal) or stained with CY3-streptavidin (1:300; Sigma) as described (Sadler et al., 2005). The left liver lobe area was measured using ImageJ.

Immunofluorescence was carried out on whole fish or on livers dissected from fixed larvae. BrdU was added to larvae water (10 mM) for 4–6 hr followed by immediate fixation, dehydration in methanol, rehydration to PBST, and permeabilization with 10 μ g/ml Proteinase K. DNA was denatured in 1 or 2 N HCl, renatured, and blocked in 10% FBS or 1% BSA in PBST prior to immunofluorescence. DNA was stained with Hoechst 33342 (Sigma). A Leica SP5 DM confocal microscope was used for imaging.

Slot Blots

Genomic DNA was denatured in 0.4 M NaOH at 95°C for 10 min and neutralized in an equal volume of cold 2 M ammonium acetate, and 100 ng DNA was blotted in duplicate onto nitrocellulose membrane using a slot blot apparatus, washed in 2 \times saline sodium citrate, and vacuum baked at 80°C for 2 hr. Half was stained with 0.2% methylene blue in 0.3 M NaOAc and the other with anti-5MeC followed by horseradish peroxidase-conjugated anti-mouse (1:2,000) and visualized by Chemiluminescence (Roche). Image J was used to quantify 5MeC and methylene blue intensity, and 5MeC levels were determined by normalizing to total DNA.

Cell Culture

Primary mouse hepatocytes were isolated and plated in triplicate at 50% confluence and then treated with 5 μ m 5-Aza or DMSO for 24 hr, and RNA was isolated.

NIH 3T3 cells were transfected in triplicate with pCDNA3.1 lacking an insert (control) or containing human RAS, UHRF1, or both and were retransfected 24 hr later. Forty-eight hours after the second transfection, 700 mg /ml neomycin was added for 7 days. Ten thousand cells per condition were plated on 0.3% soft agar layered on top of 0.6% soft agar. Media was changed every third day for 2 weeks, plates were stained with 0.005% crystal violet, and colony number was counted.

HepG2 cells cultured in DMEM supplemented with 10% (v/v) FBS and 5% (w/v) penicillin-streptomycin were transfected twice, 24 hr apart, with 20 nM siRNA-targeting firefly luciferase (GL2; Dharmacon) or UHRF1-targeting si-A and si-B using RNAiMAX (Invitrogen) as described (Tien et al., 2011).

Human Tissue Samples

Pathologically staged human tumors, dysplastic foci, and normal liver samples were obtained from the HCC Genomic Consortium (Mount Sinai Hospital, Instituto Nazionale dei Tumori, and Hospital Clinic). The study was approved by the institutional review board of each institution, and informed consent was obtained from all participants. TaqMan probes were used to analyze *UHRF1* expression by qPCR as described (Villanueva et al., 2008). Samples were grouped into a training set (nine normal liver, 18 low- and high-grade dysplastic nodules, and 40 pathologically staged HCCs; Llovet et al., 2006; Wurmbach et al., 2007) and a validation set (seven normal liver and 69 HCC; Villanueva et al., 2008). Integrative genomic and clinical data analysis was performed on 71 of the hepatitis-C-related, surgically treated HCC patients (National Center for Biotechnology Information [NCBI] Gene Expression Omnibus accession numbers GSE9829 and GSE44970). The liver pathologist, S.T., scored UHRF1 staining of 52 paraffin-embedded tumors from the training set.

Bioinformatics and Statistical Analysis

Seventy-one patients with HCC were grouped based on the median expression level of UHRF1 in the tumors determined by qPCR (UHRF1-high: n = 35 or low: n = 36). Presence of aggressive human HCC gene signatures (Table S1) were evaluated in the transcriptome data set using nearest-template prediction method (Hoshida, 2010) implemented by the GenePattern genomic analysis tool kit (<http://www.broadinstitute.org/genepattern>) based on prediction confidence $p < 0.05$. The senescence-related TP53 target genes were obtained from Molecular Signature Database (MSigDB; <http://www.broadinstitute.org/msigdb>; TANG_SENESCENCE_TP53_TARGETS_UP and _DN; Tang et al., 2007) and from NCBI Gene Expression Omnibus (GSE39469; Lujambio et al., 2013). Mouse genes from normalized microarray data were converted to human orthologs based on a mapping table (<http://www.informatics.jax.org>). Differentially expressed genes between senescent and proliferative cells were identified by using Bayesian t test implemented in Cyber-T software (<http://molgen51.biol.rug.nl/cybert>) at the significance threshold of posterior probability of differential expression >0.998 after excluding less variable genes with coefficient of variation ≤ 0.1 across the samples. Expression pattern of each signature was assessed by nearest-template prediction algorithm. Significance of induction or suppression of each signature was quantitatively measured by nominal p value of cosine distance. Pearson correlation test determined the significance between induction and suppression of gene signatures with *UHRF1* mRNA expression level as measured by qPCR. Statistical difference between groups was assessed by Wilcoxon rank-sum test and Fisher's exact test for continuous and categorical variables, respectively. Bonferroni correction for multiple hypothesis testing was applied when appropriate.

Survival analysis was performed by using Kaplan-Meier estimator and log rank test. All analyses were performed using R statistical package (<http://www.r-project.org>) and GenePattern genomic analysis tool kit (<http://www.broadinstitute.org/genepattern>). Gene expression levels and liver size were compared using Student's t or Mann Whitney U tests.

(D) Proportion of genes with DNA copy number loss according to *UHRF1* expression and *TP53* mutation status.

(E) *UHRF1* expression is significantly higher in tumors with *TP53* mutations.

(F) *DNMT1* expression by microarray analysis is significantly correlated with *UHRF1* expression assessed by qPCR in HCCs. In box and whisker plots, boxes represent the 75th and 25th percentiles, the whiskers represent the most extreme data points within interquartile range $\times 1.5$, and the horizontal bar represents the median.

See also Figure S6 and Tables S1, S2, S3, S4, S5, and S6.

ACCESSION NUMBERS

Data from RNA-seq was deposited in the NCBI Gene Expression Omnibus with accession number GSE52605.

SUPPLEMENTAL INFORMATION

Supplemental Information includes Supplemental Experimental Procedures, six figures, and six tables and can be found with this article online at <http://dx.doi.org/10.1016/j.ccr.2014.01.003>.

AUTHOR CONTRIBUTIONS

R.M., Y.H., Y.C., A.V., C.U., J.M.L. and K.C.S. conceived of the experiments; R.M., Y.H., Y.C., V.J., A.V., A.L., A.D., and S.S. carried out experiments and analyzed data; M.I.F., X.C., K.K., S.T., R.T.B., K.R., C.A., R.S., C.U., J.M.L., and K.C.S. analyzed and interpreted data; and R.M. and K.C.S. wrote the paper. Y.H. and Y.C. contributed equally.

ACKNOWLEDGMENTS

Financial support was provided by The Breast Cancer Alliance and the March of Dimes (to K.C.S.), a Pilot Project from the DFCI NCI Cancer Center (5P30CA006516-45) and The Sidney A. Swensrud Foundation (to C.U.), the NIH (5R01DK080789-02 to C.U. and K.C.S., 1R01DK099558 to Y.H., 1R01DK076986 to J.M.L., F30DK094503 to V.J., and T32CA078207-14 to Y.C.), the European Commission Seventh Framework Programme FP7-Health 2010 (Heptromic number 259744 to Y.H. and J.M.L.), The Samuel Waxman Cancer Research Foundation, The Spanish National Health Institute (SAF-2010-16055), and the Asociación Española Contra el Cáncer (to J.M.L.). Liz Loughlin, Brandon Kent, Meghan Walsh, Alex Mir, Laia Cabellos, Helena Cornellà Vives, and Sara Toffanin provided expert technical assistance. We are grateful to Sam Sidi for *tp53^{-/-}* fish, stimulating discussions, and critical reading of the manuscript.

Received: March 9, 2013

Revised: August 29, 2013

Accepted: January 6, 2014

Published: January 30, 2014

REFERENCES

- Anderson, R.M., Bosch, J.A., Goll, M.G., Hesselson, D., Dong, P.D., Shin, D., Chi, N.C., Shin, C.H., Schlegel, A., Halpern, M., and Stainier, D.Y. (2009). Loss of Dnmt1 catalytic activity reveals multiple roles for DNA methylation during pancreas development and regeneration. *Dev. Biol.* 334, 213–223.
- Arita, K., Ariyoshi, M., Tochio, H., Nakamura, Y., and Shirakawa, M. (2008). Recognition of hemi-methylated DNA by the SRA protein UHRF1 by a base-flipping mechanism. *Nature* 455, 818–821.
- Avvakumov, G.V., Walker, J.R., Xue, S., Li, Y., Duan, S., Bronner, C., Arrowsmith, C.H., and Dhe-Paganon, S. (2008). Structural basis for recognition of hemi-methylated DNA by the SRA domain of human UHRF1. *Nature* 455, 822–825.
- Babbio, F., Pistore, C., Curti, L., Castiglioni, I., Kunderfranco, P., Brino, L., Oudet, P., Seiler, R., Thalman, G.N., Roggero, E., et al. (2012). The SRA protein UHRF1 promotes epigenetic crosstalks and is involved in prostate cancer progression. *Oncogene* 31, 4878–4887.
- Berdasco, M., and Esteller, M. (2010). Aberrant epigenetic landscape in cancer: how cellular identity goes awry. *Dev. Cell* 19, 698–711.
- Berghmans, S., Murphrey, R.D., Wienholds, E., Neuberg, D., Kutok, J.L., Fletcher, C.D., Morris, J.P., Liu, T.X., Schulte-Merker, S., Kanki, J.P., et al. (2005). *tp53* mutant zebrafish develop malignant peripheral nerve sheath tumors. *Proc. Natl. Acad. Sci. USA* 102, 407–412.
- Biniszkiewicz, D., Gribnau, J., Ramsahoye, B., Gaudet, F., Eggan, K., Humpherys, D., Mastrangelo, M.A., Jun, Z., Walter, J., and Jaenisch, R. (2002). Dnmt1 overexpression causes genomic hypermethylation, loss of imprinting, and embryonic lethality. *Mol. Cell. Biol.* 22, 2124–2135.
- Bostick, M., Kim, J.K., Esteve, P.O., Clark, A., Pradhan, S., and Jacobsen, S.E. (2007). UHRF1 plays a role in maintaining DNA methylation in mammalian cells. *Science* 317, 1760–1764.
- Calvisi, D.F., Ladu, S., Gorden, A., Farina, M., Lee, J.S., Conner, E.A., Schroeder, I., Factor, V.M., and Thorgerisson, S.S. (2007). Mechanistic and prognostic significance of aberrant methylation in the molecular pathogenesis of human hepatocellular carcinoma. *J. Clin. Invest.* 117, 2713–2722.
- Cheah, M.S., Wallace, C.D., and Hoffman, R.M. (1984). Hypomethylation of DNA in human cancer cells: a site-specific change in the c-myc oncogene. *J. Natl. Cancer Inst.* 73, 1057–1065.
- Chen, T., Hevi, S., Gay, F., Tsujimoto, N., He, T., Zhang, B., Ueda, Y., and Li, E. (2007). Complete inactivation of DNMT1 leads to mitotic catastrophe in human cancer cells. *Nat. Genet.* 39, 391–396.
- Chiang, D.Y., Villanueva, A., Hoshida, Y., Peix, J., Newell, P., Minguez, B., LeBlanc, A.C., Donovan, D.J., Thung, S.N., Solé, M., et al. (2008). Focal gains of VEGFA and molecular classification of hepatocellular carcinoma. *Cancer Res.* 68, 6779–6788.
- Chu, J., Loughlin, E.A., Gaur, N.A., SenBanerjee, S., Jacob, V., Monson, C., Kent, B., Oranu, A., Ding, Y., Ukomadu, C., and Sadler, K.C. (2012). UHRF1 phosphorylation by cyclin A2/cyclin-dependent kinase 2 is required for zebrafish embryogenesis. *Mol. Biol.* 23, 59–70.
- Chu, J., Mir, A., Gao, N., Rosa, S., Monson, C., Sharma, V., Steet, R., Freeze, H.H., Lehrman, M.A., and Sadler, K.C. (2013). A zebrafish model of congenital disorders of glycosylation with phosphomannose isomerase deficiency reveals an early opportunity for corrective mannose supplementation. *Dis. Model. Mech.* 6, 95–105.
- Decottignies, A., and d'Adda di Fagagna, F. (2011). Epigenetic alterations associated with cellular senescence: a barrier against tumorigenesis or a red carpet for cancer? *Semin. Cancer Biol.* 21, 360–366.
- Di Micco, R., Sulli, G., Dobreva, M., Lontos, M., Botrugno, O.A., Gargiulo, G., dal Zuffo, R., Matti, V., d'Ario, G., Montani, E., et al. (2011). Interplay between oncogene-induced DNA damage response and heterochromatin in senescence and cancer. *Nat. Cell Biol.* 13, 292–302.
- Du, Z., Song, J., Wang, Y., Zhao, Y., Guda, K., Yang, S., Kao, H.Y., Xu, Y., Willis, J., Markowitz, S.D., et al. (2010). DNMT1 stability is regulated by proteins coordinating deubiquitination and acetylation-driven ubiquitination. *Sci. Signal.* 3, ra80.
- Eden, A., Gaudet, F., Waghmare, A., and Jaenisch, R. (2003). Chromosomal instability and tumors promoted by DNA hypomethylation. *Science* 300, 455.
- Fairweather, D.S., Fox, M., and Margison, G.P. (1987). The in vitro lifespan of MRC-5 cells is shortened by 5-azacytidine-induced demethylation. *Exp. Cell Res.* 168, 153–159.
- Feng, S., Cokus, S.J., Zhang, X., Chen, P.Y., Bostick, M., Goll, M.G., Hetzel, J., Jain, J., Strauss, S.H., Halpern, M.E., et al. (2010). Conservation and divergence of methylation patterning in plants and animals. *Proc. Natl. Acad. Sci. USA* 107, 8689–8694.
- Gaudet, F., Hodgson, J.G., Eden, A., Jackson-Grusby, L., Dausman, J., Gray, J.W., Leonhardt, H., and Jaenisch, R. (2003). Induction of tumors in mice by genomic hypomethylation. *Science* 300, 489–492.
- Gaudet, F., Rideout, W.M., 3rd, Meissner, A., Dausman, J., Leonhardt, H., and Jaenisch, R. (2004). Dnmt1 expression in pre- and postimplantation embryogenesis and the maintenance of IAP silencing. *Mol. Cell. Biol.* 24, 1640–1648.
- Hashimoto, H., Horton, J.R., Zhang, X., Bostick, M., Jacobsen, S.E., and Cheng, X. (2008). The SRA domain of UHRF1 flips 5-methylcytosine out of the DNA helix. *Nature* 455, 826–829.
- Hoshida, Y. (2010). Nearest template prediction: a single-sample-based flexible class prediction with confidence assessment. *PLoS ONE* 5, e15543.
- Howard, G., Eiges, R., Gaudet, F., Jaenisch, R., and Eden, A. (2008). Activation and transposition of endogenous retroviral elements in hypomethylation induced tumors in mice. *Oncogene* 27, 404–408.

- Imrie, D., and Sadler, K.C. (2010). White adipose tissue development in zebrafish is regulated by both developmental time and fish size. *Dev. Dyn.* 239, 3013–3023.
- Jackson-Grusby, L., Beard, C., Possemato, R., Tudor, M., Fambrough, D., Csankovszki, G., Dausman, J., Lee, P., Wilson, C., Lander, E., and Jaenisch, R. (2001). Loss of genomic methylation causes p53-dependent apoptosis and epigenetic deregulation. *Nat. Genet.* 27, 31–39.
- Jin, W., Chen, L., Chen, Y., Xu, S.G., Di, G.H., Yin, W.J., Wu, J., and Shao, Z.M. (2010). UHRF1 is associated with epigenetic silencing of BRCA1 in sporadic breast cancer. *Breast Cancer Res. Treat.* 123, 359–373.
- Jirtle, R.L. (2004). IGF2 loss of imprinting: a potential heritable risk factor for colorectal cancer. *Gastroenterology* 126, 1190–1193.
- Karpf, A.R., and Matsui, S. (2005). Genetic disruption of cytosine DNA methyltransferase enzymes induces chromosomal instability in human cancer cells. *Cancer Res.* 65, 8635–8639.
- Karpf, A.R., Moore, B.C., Ririe, T.O., and Jones, D.A. (2001). Activation of the p53 DNA damage response pathway after inhibition of DNA methyltransferase by 5-aza-2'-deoxycytidine. *Mol. Pharmacol.* 59, 751–757.
- Kwan, K.M., Fujimoto, E., Grabher, C., Mangum, B.D., Hardy, M.E., Campbell, D.S., Parant, J.M., Yost, H.J., Kanki, J.P., and Chien, C.B. (2007). The Tol2kit: a multisite gateway-based construction kit for Tol2 transposon transgenesis constructs. *Dev. Dyn.* 236, 3088–3099.
- Li, E., Beard, C., and Jaenisch, R. (1993). Role for DNA methylation in genomic imprinting. *Nature* 366, 362–365.
- Liu, X., Gao, Q., Li, P., Zhao, Q., Zhang, J., Li, J., Koseki, H., and Wong, J. (2013). UHRF1 targets DNMT1 for DNA methylation through cooperative binding of hemi-methylated DNA and methylated H3K9. *Nat. Commun.* 4, 1563.
- Llovet, J.M., Burroughs, A., and Bruix, J. (2003). Hepatocellular carcinoma. *Lancet* 362, 1907–1917.
- Llovet, J.M., Chen, Y., Wurmbach, E., Roayaie, S., Fiel, M.I., Schwartz, M., Thung, S.N., Khitrov, G., Zhang, W., Villanueva, A., et al. (2006). A molecular signature to discriminate dysplastic nodules from early hepatocellular carcinoma in HCV cirrhosis. *Gastroenterology* 131, 1758–1767.
- Llovet, J.M., Ricci, S., Mazzaferro, V., Hilgard, P., Gane, E., Blanc, J.F., de Oliveira, A.C., Santoro, A., Raoul, J.L., Forner, A., et al.; SHARP Investigators Study Group (2008). Sorafenib in advanced hepatocellular carcinoma. *N. Engl. J. Med.* 359, 378–390.
- Lujambio, A., Akkari, L., Simon, J., Grace, D., Tschaharganeh, D.F., Bolden, J.E., Zhao, Z., Thapar, V., Joyce, J.A., Krizhanovsky, V., and Lowe, S.W. (2013). Non-cell-autonomous tumor suppression by p53. *Cell* 153, 449–460.
- McDuff, F.K., and Turner, S.D. (2011). Jailbreak: oncogene-induced senescence and its evasion. *Cell. Signal.* 23, 6–13.
- Mudbhary, R., and Sadler, K.C. (2011). Epigenetics, development, and cancer: zebrafish make their mark. *Birth Defects Res. C Embryo Today* 93, 194–203.
- Nishiyama, A., Yamaguchi, L., Sharif, J., Johmura, Y., Kawamura, T., Nakanishi, K., Shimamura, S., Arita, K., Kodama, T., Ishikawa, F., et al. (2013). Uhrf1-dependent H3K23 ubiquitylation couples maintenance DNA methylation and replication. *Nature* 502, 249–253.
- Pogribny, I.P., and Rusyn, I. (2014). Role of epigenetic aberrations in the development and progression of human hepatocellular carcinoma. *Cancer Lett.* 342, 223–230.
- Qin, W., Leonhardt, H., and Spada, F. (2011). Usp7 and Uhrf1 control ubiquitination and stability of the maintenance DNA methyltransferase Dnmt1. *J. Cell. Biochem.* 112, 439–444.
- Rai, K., Nadauld, L.D., Chidester, S., Manos, E.J., James, S.R., Karpf, A.R., Cairns, B.R., and Jones, D.A. (2006). Zebra fish Dnmt1 and Suv39h1 regulate organ-specific terminal differentiation during development. *Mol. Cell. Biol.* 26, 7077–7085.
- Rai, K., Sarkar, S., Broadbent, T.J., Voas, M., Grossmann, K.F., Nadauld, L.D., Dehghanizadeh, S., Hagos, F.T., Li, Y., Toth, R.K., et al. (2010). DNA demethylase activity maintains intestinal cells in an undifferentiated state following loss of APC. *Cell* 142, 930–942.
- Sadler, K.C., Amsterdam, A., Soroka, C., Boyer, J., and Hopkins, N. (2005). A genetic screen in zebrafish identifies the mutants vps18, nf2 and foie gras as models of liver disease. *Development* 132, 3561–3572.
- Sadler, K.C., Krahn, K.N., Gaur, N.A., and Ukomadu, C. (2007). Liver growth in the embryo and during liver regeneration in zebrafish requires the cell cycle regulator, Uhrf1. *Proc. Natl. Acad. Sci. USA* 104, 1570–1575.
- Sharif, J., Muto, M., Takebayashi, S., Suetake, I., Iwamatsu, A., Endo, T.A., Shinga, J., Mizutani-Koseki, Y., Toyoda, T., Okamura, K., et al. (2007). The SRA protein Np95 mediates epigenetic inheritance by recruiting Dnmt1 to methylated DNA. *Nature* 450, 908–912.
- Tang, X., Milyavsky, M., Goldfinger, N., and Rotter, V. (2007). Amyloid-beta precursor-like protein APLP1 is a novel p53 transcriptional target gene that augments neuroblastoma cell death upon genotoxic stress. *Oncogene* 26, 7302–7312.
- Taylor, E.M., Bonsu, N.M., Price, R.J., and Lindsay, H.D. (2013). Depletion of Uhrf1 inhibits chromosomal DNA replication in Xenopus egg extracts. *Nucleic Acids Res.* 41, 7725–7737.
- Tien, A.L., Senbanerjee, S., Kulkarni, A., Mudbhary, R., Goudreau, B., Ganesan, S., Sadler, K.C., and Ukomadu, C. (2011). UHRF1 depletion causes a G2/M arrest, activation of DNA damage response and apoptosis. *Biochem. J.* 435, 175–185.
- Tischoff, I., and Tannapape, A. (2008). DNA methylation in hepatocellular carcinoma. *World J. Gastroenterol.* 14, 1741–1748.
- Tittle, R.K., Sze, R., Ng, A., Nuckles, R.J., Swartz, M.E., Anderson, R.M., Bosch, J., Stainier, D.Y., Eberhart, J.K., and Gross, J.M. (2011). Uhrf1 and Dnmt1 are required for development and maintenance of the zebrafish lens. *Dev. Biol.* 350, 50–63.
- Unoki, M., Daigo, Y., Koinuma, J., Tsuchiya, E., Hamamoto, R., and Nakamura, Y. (2010). UHRF1 is a novel diagnostic marker of lung cancer. *Br. J. Cancer* 103, 217–222.
- Ventura, A., Kirsch, D.G., McLaughlin, M.E., Tuveson, D.A., Grimm, J., Lintault, L., Newman, J., Reczek, E.E., Weissleder, R., and Jacks, T. (2007). Restoration of p53 function leads to tumour regression in vivo. *Nature* 445, 661–665.
- Villanueva, A., Chiang, D.Y., Newell, P., Peix, J., Thung, S., Alsinet, C., Tovar, V., Roayaie, S., Minguez, B., Sole, M., et al. (2008). Pivotal role of mTOR signaling in hepatocellular carcinoma. *Gastroenterology* 135, 1972–1983.
- Villanueva, A., Hoshida, Y., Battiston, C., Tovar, V., Sia, D., Alsinet, C., Cornellà, H., Liberzon, A., Kobayashi, M., Kumada, H., et al. (2011). Combining clinical, pathology, and gene expression data to predict recurrence of hepatocellular carcinoma. *Gastroenterology* 140, 1501–1512.
- Wang, F., Yang, Y.Z., Shi, C.Z., Zhang, P., Moyer, M.P., Zhang, H.Z., Zou, Y., and Qin, H.L. (2012). UHRF1 promotes cell growth and metastasis through repression of p16(ink4a) in colorectal cancer. *Ann. Surg. Oncol.* 19, 2753–2762.
- Weber, M., and Schübeler, D. (2007). Genomic patterns of DNA methylation: targets and function of an epigenetic mark. *Curr. Opin. Cell Biol.* 19, 273–280.
- Wurmbach, E., Chen, Y.B., Khitrov, G., Zhang, W., Roayaie, S., Schwartz, M., Fiel, I., Thung, S., Mazzaferro, V., Bruix, J., et al. (2007). Genome-wide molecular profiles of HCV-induced dysplasia and hepatocellular carcinoma. *Hepatology* 45, 938–947.
- Xue, W., Zender, L., Miethling, C., Dickins, R.A., Hernando, E., Krizhanovsky, V., Cordon-Cardo, C., and Lowe, S.W. (2007). Senescence and tumour clearance is triggered by p53 restoration in murine liver carcinomas. *Nature* 445, 656–660.
- Yamada, Y., Jackson-Grusby, L., Linhart, H., Meissner, A., Eden, A., Lin, H., and Jaenisch, R. (2005). Opposing effects of DNA hypomethylation on intestinal and liver carcinogenesis. *Proc. Natl. Acad. Sci. USA* 102, 13580–13585.
- You, J.S., and Jones, P.A. (2012). Cancer genetics and epigenetics: two sides of the same coin? *Cancer Cell* 22, 9–20.